

1

Supplementary Information

2 **A combined experimental and theoretical approach towards mechano-** 3 **phenotyping of biological cells using a constricted microchannel**

4 A. Raj¹, M. Dixit², M. Doble², A. K. Sen^{1,*}

5 ¹Department of Mechanical Engineering, Indian Institute of Technology Madras, Chennai-600036, India

6 ²Department of Biotechnology, Indian Institute of Technology Madras, Chennai-600036, India

7

8 *Author to whom correspondence should be addressed. Email: ashis@iitm.ac.in

9

10 **S.1 Theoretical model**

11 **S.1.1 Entry of a cell into a micro-constriction**

12 In order to model the cell entry into the micro-constriction, we have utilized the theoretical model derived by Tsai et al.¹
13 which is explained below. The basic assumption for the modelling are as follows. The cytoplasmic flow is axisymmetric and
14 the cell body outside the micro-constriction is spherical. Initially the cytoplasm flow is modelled as a plug flow with isotropic
15 and incompressible conditions applied. For low Reynolds number flow, the basic continuity and conservation of momentum
16 equation governing the cytoplasmic flow are given as

$$17 \quad \nabla \cdot \vec{V} = 0 \quad (1)$$

$$18 \quad \mu \nabla^2 \vec{V} = \Delta p \quad (2)$$

19 where, \vec{V} is the velocity vector, μ is the cytoplasmic viscosity and p is the hydrostatic pressure. By introducing the spherical
20 coordinate system, the velocity components V_r and V_θ can be represented in terms of stream function $\psi(r, \theta)$ as follows,

$$21 \quad V_r = -\frac{1}{r^2 \sin \theta} \frac{\partial \psi}{\partial \theta} \quad (3)$$

$$22 \quad V_\theta = \frac{1}{r \sin \theta} \frac{\partial \psi}{\partial r} \quad (4)$$

23 Applying equations 3 and 4 to Eqn. 2, we get:

$$24 \quad E^4 \psi = 0 \quad (5)$$

25 where, the operator E^2 is defined as $E^2 = \frac{\partial^2}{\partial r^2} + \frac{1-\zeta^2}{r^2} \frac{\partial^2}{\partial \zeta^2}$, and $\zeta = \cos \theta$. The general solution to Eqn. 5 is given

26 by ²:

$$27 \quad \psi = \sum_{n=2}^{\infty} (A_n r^n + C_n r^{n+2}) I_n(\zeta) \quad (6)$$

28 where, A_n and C_n are coefficients which can be determined by applying boundary conditions and $I_n(\zeta)$ are Gegenbauer
29 functions of first kind given by

$$30 \quad I_n(\zeta) = \frac{P_{n-2}(\zeta) - P_n(\zeta)}{2n-1} \quad (7)$$

31 and $P_n(\zeta)$ are the Legendre polynomials. Based on the assumptions stated above, stress boundary conditions are given as

$$32 \quad \sigma_{r\theta} = 0 \quad (8)$$

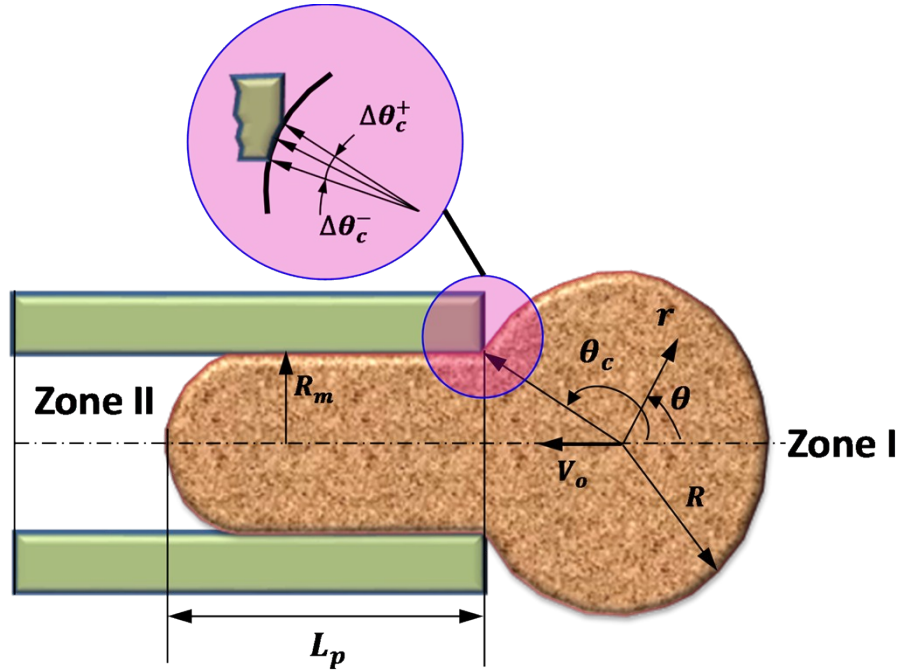
33

34

35

$$\sigma_{rr} = \begin{cases} -(P_a + \frac{2T}{R}) & \text{for } \zeta_c + k < \zeta \leq 1 \\ -h & \text{for } \zeta_c - k < \zeta \leq \zeta_c + k \\ -(P_p + \frac{2T}{R}) & \text{for } -1 \leq \zeta < \zeta_c - k \end{cases} \quad (9)$$

6 where, $\sigma_{r\theta}$ and σ_{rr} are shear and normal stresses on the boundary, respectively, R is the instantaneous cell radius, R_f is
7 the radius of the cell projection inside the constriction, P_a is the pressure in the Zone I (Fig. S1) upstream of the cell outside
8 the micro-constriction channel, P_p is the pressure in the micro-constriction downstream the cell in Zone II (Fig. S1), T is the
9 cortical tension of the cell membrane, $\zeta_c = \cos \theta_c$, $k = \zeta_c - \cos(\theta_c + \Delta\theta_c^-) = \cos(\theta_c - \Delta\theta_c^+) - \zeta_c$, and h is the
10 uniform reaction stress from the constriction in the finite contact area between the cell and the pipette (Fig.S1). The typical
11 value of k is reported to be around 0.1 in the literature ¹.



12
13 **Fig. S1** Schematic of a single cell entering into a micro-constriction at a fixed pressure gradient.

14
15 For a Newtonian fluid, the constitutive relations between the stress component and flow-field can be given as

$$\sigma_{rr} = -p + 2\mu \frac{\partial V_r}{\partial r} \quad (10)$$

$$\sigma_{r\theta} = \mu \left[\frac{1}{r} \frac{\partial V_r}{\partial \theta} + r \frac{\partial}{\partial r} \left(\frac{V_\theta}{r} \right) \right] \quad (11)$$

18
19 By incorporating boundary conditions (Eqn. 8 and 9) into Eqns. 10 and 11 and solving for velocity components gives

$$V_r = -V_o \zeta + \frac{\Delta p R}{4\mu} \sum_{n=3}^{\infty} \left[n \left(\frac{r}{R} \right)^n - \frac{n^2 - 1}{n - 2} \left(\frac{r}{R} \right)^{n-2} \right] f_n(\zeta_c, k) P_{n-1}(\zeta) \quad (12)$$

$$V_\theta = V_o \sin \theta - \frac{\Delta p R}{4\mu} \sum_{n=3}^{\infty} n \left[(n+2) \left(\frac{r}{R} \right)^n - \frac{n^2-1}{n-2} \left(\frac{r}{R} \right)^{n-2} \right] f_n(\zeta_c, k) \frac{I_n(\zeta)}{\sin \theta} \quad (13)$$

where V_o is the centre velocity of the spherical cell outside the micro-constriction in Zone I (Fig.S1) and given as

$$V_o = -\frac{\Delta p R}{4\mu} \sum_{n=3}^{\infty} f_n(\zeta_c, k) \left[\frac{2n-1}{n-2} \zeta_c P_{n-1}(\zeta_c) + \frac{3n}{n-2} I_n(\zeta_c) \right] \quad (14)$$

$$\text{where, } f_n(\zeta_c, k) = \frac{(2n-1)(n-1)}{2n^2+1} \left[\left(\frac{1}{2} - \frac{1-\zeta_c^2-k^2}{4\zeta_c k} \right) I_n(\zeta_c - k) + \left(\frac{1}{2} + \frac{1-\zeta_c^2-k^2}{4\zeta_c k} \right) I_n(\zeta_c + k) \right] \quad (15)$$

$$\text{and } \Delta p = (\Delta p_{cell}) \left[1 - \beta \left(\frac{R_m}{R_f} - \frac{R_m}{R} \right) \right] \quad (16)$$

In Eqn. 16, Δp_{cell} is the pressure drop applied across the cell given by $\Delta p_{cell} = p_a - p_p$, R_m is the hydraulic radius of the micro-constriction, β is given as

$$\beta = \frac{2T}{\Delta p_{cell} R_m} \quad (17)$$

The deformation rate tensor components can be given as

$$\epsilon_{ij} = \frac{\Delta p_{cell}}{4\mu} \left[1 - \beta \left(\frac{R_m}{R_f} - \frac{R_m}{R} \right) \right] \hat{\epsilon}_{ij} \quad (18)$$

where, $\hat{\epsilon}_{ij}$ are determined from Eqns. 12-14 as:

$$\hat{\epsilon}_{rr} = \sum_{n=3}^{\infty} \left[n^2 \left(\frac{r}{R} \right)^2 - (n^2-1) \right] \left(\frac{r}{R} \right)^{n-3} f_n(\zeta_c, k) P_{n-1}(\zeta) \quad (19)$$

$$\hat{\epsilon}_{r\theta} = \left[1 - \left(\frac{r}{R} \right)^2 \right] \sum_{n=3}^{\infty} \left[n^2(n^2-1) \right] \left(\frac{r}{R} \right)^{n-3} f_n(\zeta_c, k) \frac{I_n(\zeta)}{\sin \theta} \quad (20)$$

$$\hat{\epsilon}_{\theta\theta} = \left\{ - \sum_{n=3}^{\infty} (n+1) \left[n \left(\frac{r}{R} \right)^2 - \frac{(n-1)^2}{n-2} \right] \left(\frac{r}{R} \right)^{n-3} f_n(\zeta_c, k) P_{n-1}(\zeta) + \frac{\zeta}{1-\zeta^2} \sum_{n=3}^{\infty} n \left[(n+2) \left(\frac{r}{R} \right)^2 - \frac{(n-1)^2}{n-2} \right] \left(\frac{r}{R} \right)^{n-3} f_n(\zeta_c, k) I_n(\zeta) \right\} \quad (21)$$

$$\hat{\epsilon}_{\phi\phi} = \left\{ \sum_{n=3}^{\infty} \left[n \left(\frac{r}{R} \right)^2 - \frac{(n-1)^2}{n-2} \right] \left(\frac{r}{R} \right)^{n-3} f_n(\zeta_c, k) P_{n-1}(\zeta) - \frac{\zeta}{1-\zeta^2} \sum_{n=3}^{\infty} n \left[(n+2) \left(\frac{r}{R} \right)^2 - \frac{(n-1)^2}{n-2} \right] \left(\frac{r}{R} \right)^{n-3} f_n(\zeta_c, k) I_n(\zeta) \right\} \quad (22)$$

The rate of viscous energy dissipation is proportional to $\phi = \frac{1}{2} \epsilon_{ij} \epsilon_{ij}$ with $i, j = 1, 2, 3$ where ϵ_{ij} are the components of the cellular deformation rate tensor and the indices 1, 2, 3 refer to the r, θ, ϕ directions respectively. The shear rate which is a function of position within the cell and time is therefore defined as $\dot{\gamma} = \sqrt{\phi}$. An instantaneous mean shear rate $\dot{\gamma}_a$ is defined as an average of ϕ over the spherical portion of the cell volume outside the micro-constriction as

$$\dot{\gamma}_a = \left[\frac{3}{2} \int_0^R \frac{r^2}{R^3} \int_0^\pi \phi \sin \theta d\theta dr \right]^{\left(\frac{1}{2}\right)}$$

$$\text{or, } \dot{\gamma}_a = \left[\frac{3}{2} \int_0^R \frac{r^2}{R^3} \int_0^\pi \left(\frac{1}{2} \epsilon_{ij} \epsilon_{ij} \right) \sin \theta d\theta dr \right]^{\left(\frac{1}{2}\right)} \quad (23)$$

Once the term ϵ_{ij} in the above equation is replaced in terms of other known parameters using Eqn. 18, the instantaneous average shear rate can be found. Now, at this point the cytoplasmic viscosity μ in the Eqn. 18 is represented in terms of the shear rate using shear thinning power law mode as follows.

The shear thinning liquid drop model assumes the cytoplasm of the cell as a non-Newtonian liquid. It accounts for the change in the viscosity of the cytoplasm with the change in the applied shear rate. The relation between cytoplasmic viscosity μ and the mean shear rate (averaged over the spherical portion outside the micro-constriction) is given by power law model as

$$\mu = \mu_o \left(\frac{\dot{\gamma}_a}{\dot{\gamma}_o} \right)^{-b} \quad (24)$$

where μ_o is the reference or, base viscosity at a characteristic shear rate $\dot{\gamma}_o$ and b is the power coefficient which represents the degree of shear thinning of the cell's cytoplasm. Since, the choice of $\dot{\gamma}_o$ is arbitrary, for convenience, we have selected

$$\dot{\gamma}_o = \frac{\Delta p_{cell}}{4\mu_o}, \text{ where } \Delta p_{cell} \text{ is the pressure drop applied across the cell.}$$

Now, coupling Eqn. 18 and 24 with the Eqn. 23, we get instantaneous average shear rate $\dot{\gamma}_a$ as follows

$$\frac{\dot{\gamma}_a}{\dot{\gamma}_o} = \left\{ \left[1 - \beta \left(\frac{R_m}{R_f} - \frac{R_m}{R} \right) \right] \Phi \right\}^{1/(1-b)} \quad (25)$$

where, the function Φ is given as

$$\Phi = \left[\frac{3}{4} \int_0^R \frac{r^2}{R^3} \int_0^\pi (\hat{\epsilon}_{rr}^2 + \hat{\epsilon}_{r\theta}^2 + \hat{\epsilon}_{\theta\theta}^2 + \hat{\epsilon}_{\phi\phi}^2) \sin \theta d\theta dr \right]^{\frac{1}{2}} \quad (26)$$

Now, using Eqn. 12 and 13, the flow rate into the constriction channel can be determined as

$$Q = \frac{\pi R_m^3 \Delta p_n (\dot{\gamma}_a)^b}{4\mu_o (\dot{\gamma}_o)^b} \left[1 - \beta \left(\frac{R_m}{R_f} - \frac{R_m}{R} \right) \right] \hat{q} \quad (27)$$

where

$$\hat{q} = \frac{R}{R_m} \left\{ \sum_{n=3}^{\infty} \frac{2n-1}{n-2} \left(\frac{r}{R} \right)^{n-2} f_n(\zeta_c, k) \left[2 \left(\frac{R}{R_m} \right)^2 I_n(\zeta_c) - \zeta_c P_{n-1}(\zeta_c) \right] - 3 \sum_{n=3}^{\infty} \frac{n}{n-2} \left(\frac{r}{R} \right)^{n-2} f_n(\zeta_c, k) I_n(\zeta_c) \right\}, \quad \frac{r}{R} \rightarrow 1 \quad (28)$$

Further, using the conservation of cell volume, cell entry velocity dL_p/dt is determined by

$$\frac{dL_p}{dt} = Q \frac{G}{\pi R_m^2} \quad (29)$$

1
2
3
4
5

Finally coupling Eqns. 25 and 27 with Eqn. 29, we get

$$\frac{dL_p}{dt} = G \frac{R_m \Delta p_{cell}}{4\mu_o} \left\{ \left[1 - \beta \left(\frac{R_m}{R_f} - \frac{R_m}{R} \right) \right] \Phi \right\}^{b/(1-b)} \left[1 - \beta \left(\frac{R_m}{R_f} - \frac{R_m}{R} \right) \right] \hat{q} \quad (30)$$

6 where G is a geometrical factor. $G = 1$ for $L_p > R_m$ and $G = \frac{2R_m^2}{R_m^2 + L_p^2}$ for $L_p \leq R_m$, Φ and \hat{q} are given by Eqns. 26 and 28
7 respectively, L_p is the projection length of the cell's leading edge into the micro-constriction, R_m is the hydraulic radius of
8 the micro-constriction channel, R_f is the radius of the cell's leading edge radius inside the microchannel, Δp_{cell} is the pressure
9 driving the cell into the micro-constriction, and R is the instantaneous radius of the cell's portion outside the micro-
10 constriction. R is related with the projection length L_p by using volume conservation for the cell. All the infinite series
11 expressions shown in Eqns. 19 to 22 and 28 were solved using MATLAB. Further the double integration in the Eqn. 26 was
12 solved numerically using composite trapezoidal rule by taking ~ 50 grid points in r and θ directions. The Eqn. 30 represents
13 the governing differential equation for the cell entry into the micro-constriction which shows the progression of cell migration
14 into the micro-constriction in terms of cell's leading edge protrusion length $L_p(t)$ with time.

15
16 The Eqn. 30 was solved numerically by using the fourth order Runge-Kutta method in MATLAB. Now, experimentally we
17 know the maximum deformed length l of a cell (of known radius), while migrating through the micro-constriction. From the
18 numerically found $L_p(t)$ profile, we find out the time $t = t_e$ at which $L_p(t = t_e) = l$, which gives us the predicted entry time
19 of a cell of known size. Hence, by incorporating the maximum deformed cell length l (for a cell of undeformed radius R_o)
20 into Eqn. 31, we can predict the entry time for the cell provided the parameters μ_o and b are known. Please note that, the cell
21 progression profile $L_p(t)$ depends on the cytoplasmic viscosity μ_o and the shear thinning coefficient b and the parameters
22 μ_o and b are cell specific. In order to obtain the fitting parameters μ_o and b , we utilize the training set of experimental data
23 and select the parameters such that the entry time predicted using theoretical modelling and the experiments (best fit data of
24 the training data set) match very well within a maximum error of 5%. We select the values of the fitting parameters for each
25 type of cell in a number of iterative steps similar to the approach utilized by an earlier work³. The value of μ_o was varied in
26 the range 0.1 to 2.0 Pa.s and b with a step size of ± 0.05 until the best match (or minimum error) between the model and
27 experimental data was observed in terms of the entry time for different cells sizes. Further, we test the validity of the fitting
28 parameters thus obtained by comparing the predicted entry time with the test set of experimental data for the same cell line
29 (please see Fig.4 of the manuscript). The predicted entry time matches well with the experimentally obtained best fit entry
30 time within a maximum error of 12%.

31

32 S.1.2 Transit of a cell in a micro-constriction

33 By solving the simplified N-S equation (as shown in eqn. 1 of the manuscript) with boundary conditions $u(r = r_c) = U_c$ and
34 $u(r = a) = 0$, the velocity profile in the annular region between the cell and wall is obtained as

35

$$u = \left(\frac{k}{4\mu_m} \right) r^2 + C_1 \ln r + C_2$$

1 where, $C_1 = \frac{\left(\frac{k}{4\mu_m}\right)(a^2 - r_c^2) + U_c}{\ln\left(\frac{r_c}{a}\right)}$ and, $C_2 = \frac{U_c \ln a + \frac{k}{4\mu_m}(a^2 \ln r_c - r_c^2 \ln a)}{\ln\left(\frac{a}{r_c}\right)}$ (31)

2 and, k is the pressure gradient applied across the cell. On utilizing the expression of velocity in the annular region with the
3 expression for Q_{leak} , we get the following expression.

4
$$\frac{k}{16\mu_m}(a^4 - r_c^4) + \left\{ \frac{2(a^2 \ln a - r_c^2 \ln r_c) - (a^2 - r_c^2)}{4} \right\} \left\{ \frac{\left(\frac{k}{4\mu}\right)(a^2 - r_c^2) + U_c}{\ln\left(\frac{r_c}{a}\right)} \right\} + \left(\frac{a^2 - r_c^2}{2} \right) \left\{ \frac{U_c \ln a + \frac{k}{4\mu}(a^2 \ln r_c - r_c^2 \ln a)}{\ln\left(\frac{a}{r_c}\right)} \right\} = \frac{Q_{leak}}{2\pi}$$
 (32)

5 Further, the velocity gradient in the annular region is found by calculating the derivative of eqn. 32 as follows.

6
$$\frac{\partial u}{\partial r} = \frac{kr_c}{2\mu_m} + \frac{\frac{k}{4\mu_m}(a^2 - r_c^2) + U_c}{r_c \ln\left(\frac{r_c}{a}\right)}$$
 (33)

7 Now, the shear stress on the cell wall surface $\tau = \tau_{rz} = -\mu_m \left(\frac{\partial u}{\partial r}\right)_{r=r_c}$ is given by

8
$$\tau = -\mu_m \left[\frac{kr_c}{2\mu_m} + \frac{\frac{k}{4\mu_m}(a^2 - r_c^2) + U_c}{r_c \ln\left(\frac{r_c}{a}\right)} \right]$$
 (34)

9 Next, by utilizing the expression relating the tension force acting on the cell membrane T and the shear stress acting on the
10 cell wall surface can be given as $T = \frac{\tau A}{l}$, where A is the surface area of the cell exposed to the media flowing around it and
11 l is the length of the deformed cell. Hence the tension force acting on the cell membrane can be expressed as

12
$$T = \frac{-A\mu_m}{l} \left[\frac{kr_c}{2\mu_m} + \frac{\frac{k}{4\mu_m}(a^2 - r_c^2) + U_c}{r_c \ln\left(\frac{r_c}{a}\right)} \right]$$
 (35)

13 S.1.3 Pressure drop across a single cell

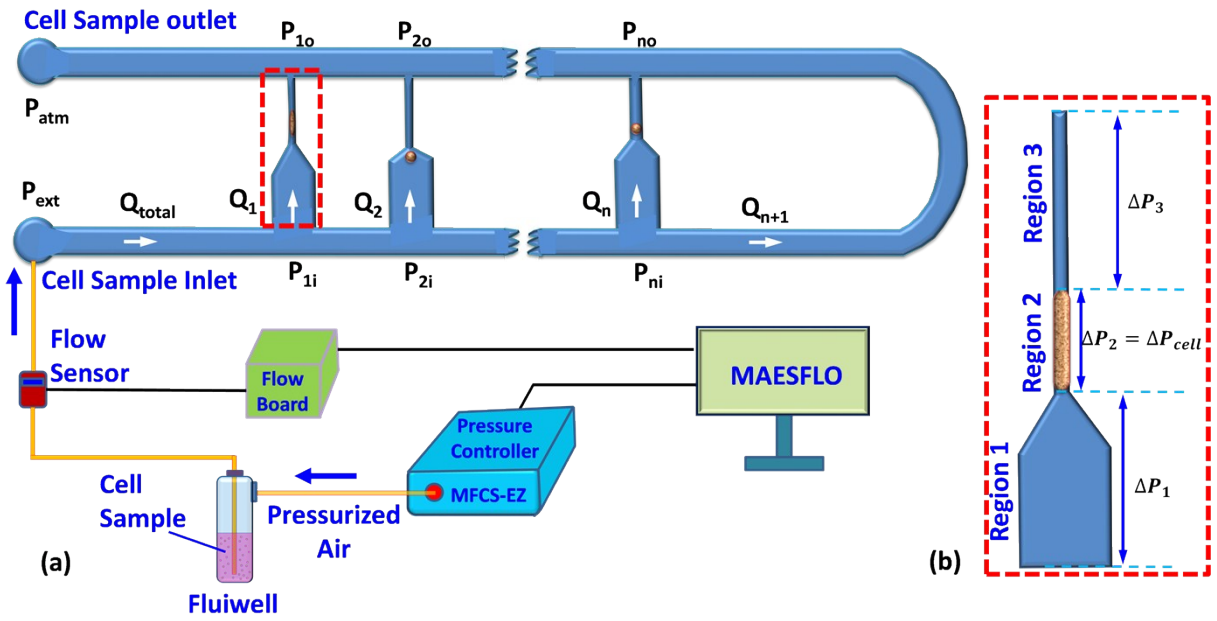
14 The schematic of the experimental setup is shown in the Fig. S2a. With the help of pressure controller and MAESFLO
15 software, the cell sample was infused into the device and the flow rate was measured using S-type flow sensors along with
16 the flow-board connected with the MAESFLO platform (Fluigent). Since the setup of the device is such that we can measure
17 the deformability of multiple cells at a time, different parallel constrictions will have single cells flowing through them during
18 the course of the measurements. This way, the hydrodynamic resistance of the device keeps changing with time as already
19 reported by earlier works dealing with parallel constrictions^{4,5}. Hence, we need to monitor the pressure across the constriction
20 carefully. For this purpose, at a certain instant when the cell is flowing through a constriction, the movement and the
21 deformation of the single cells are monitored using high-speed high resolution camera. Once U_c and ε are found, we proceed
22 with the analysis to determine pressure gradient across a single cell.

1 As shown in Fig. S2a, the total flow rate through the device Q_{total} gets distributed into Q_1, Q_2, \dots, Q_n and Q_{n+1} through the
 2 micro-constrictions and a pressure gradient of $(P_{1in} - P_{1o}), (P_{2in} - P_{2o}), \dots, \text{and } (P_{nin} - P_{no})$ gets developed across 1st, 2nd
 3 ...and nth constrictions respectively. Hence, the total flow rate Q_{total} can be written as follows.

$$4 \quad Q_{total} = Q_1 + Q_2 + \dots + Q_n + Q_{n+1} \quad (36)$$

5 Now let's consider a single constriction, say its i^{th} constriction and the flow rate through it is Q_i . The total flow rate through
 6 the micro-constriction Q_i can be given as the sum of leak flow rate Q_{leak} and the flow rate contribution from the cell flow
 7 denoted as Q_{cell} . Hence, $Q_i = Q_{cell} + Q_{leak}$, which can be written as

$$8 \quad Q_i = \pi r_c^2 U_c + \frac{\pi r_c^2 U_c (4a^2 - \pi r_c^2)}{a^2 (\pi \varepsilon - 1) + \pi r_c^2} \quad (37)$$



9
 10 **Fig. S2** (a) Schematic of the experimental setup, (b) Regions specified in a single constriction.

11 Further r_c is expressed in terms of $k_i = \Delta P_{cell}/l$ and U_c as follows,

$$12 \quad \frac{r_c^2 (4a^2 - \pi r_c^2) U_c}{2 \{ a^2 (\pi \varepsilon - 1) + \pi r_c^2 \}} - \frac{k_i (a^2 - r_c^2) + U_c}{4 \mu_m} \left[(a^2 \ln a - r_c^2 \ln r_c) - (a^2 - r_c^2) \right] - \frac{U_c \ln a + \frac{k}{4 \mu} (a^2 \ln r_c - r_c^2 \ln a)}{2 \ln(a/r_c)} (a^2 - r_c^2) = \frac{k_i (a^4 - r_c^4)}{16 \mu_m} \quad (38)$$

14 The cell sample was infused through the microchannel using a constant pressure device. A constant pressure Δp_{ext} was
 15 applied across the device. When a cell passes through the constriction the region of the microchannel can be divided into
 16 three zones namely region 1, 2 and 3 (Fig.S2 (b)). First and third region are the regions of the microchannel which contain
 17 only media sample (or, very low concentrated sample such that it does not affect the overall hydrodynamic resistance of the
 18 channel) and region 2 contains a deformed cell. The pressure across the constriction will be distributed in the regions specified
 19 and can be written as,

$$20 \quad P_{iin} - P_{io} = \Delta p_1 + (\Delta p_{cell})_i + \Delta p_3 \quad (39)$$

21 where, Δp_1 and Δp_3 can be represented in terms of Q_i , μ_m and the channel dimensions using Hagen-Poiseuille's law for
 22 rectangular microchannel. Similarly, equations 36 to 39 are valid for all the constriction channels.

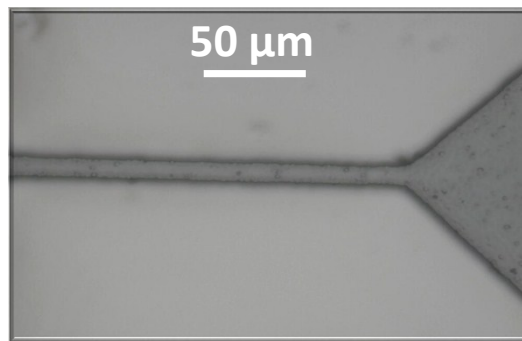
1 The entire flow network is converted into hydrodynamic resistance network and solved for finding out the pressure gradient
 2 applied across the cell Δp_{cell} as well as flow rate Q_i through the micro-constriction by using Kirchoff's law. The main
 3 challenge here lies in finding out the unknown hydrodynamic resistance of the micro-constriction branch of the hydrodynamic
 4 resistance network. This issue is resolved as explained below. The hydrodynamic resistance of the i^{th} micro-constriction
 5 branch of the network (say R_i) can be given as

$$R_i = \left(\frac{P_{iin} - P_{io}}{Q_i} \right) = \left(\frac{\Delta p_1 + k_i \cdot l + \Delta p_3}{Q_i} \right) \quad (40)$$

6
 7 Combining eqn. 37 & 38, we get Q_i in terms of pressure gradient k (U_c is measured from experimented and incorporated),
 8 which is incorporated in the eqn. 40 and hence we get the hydrodynamic resistance R_i of the micro-constriction branch in
 9 terms of k_i . Once R_i is expressed in terms of k_i , the whole hydrodynamic resistance network has only unknowns remaining
 10 in terms of pressure gradient across the micro-constriction and the flows across them, which is solved using Kirchoff's law.
 11 Hence, in summary, eqns. 36-40 coupled together with the Kirchoff's law solves the purpose of finding out the pressure
 12 gradient across a single cell.

13 S.2 Device Fabrication

14 The PDMS microchannel devices were fabricated using Standard soft lithography process. First of all, a flexi mask was
 15 designed in AutoCAD LT 2008 and printed at 40000 dpi. (Fine Line imaging, USA). Then, a 4" silicon wafer (semiconductor
 16 Technology and Application, Milpitas, USA) was cleaned using HF dip followed by DI water rinse and placed in oven for 2
 17 min at 120° C to remove moisture. Next, the wafer was spun coated with photoresist SU8-10 (Micro Chem Corp, Newton,
 18 USA) at 3000 rpm for 30 s with an acceleration of 300 rpm/s. Further, spun coated wafer was Soft baked at 65° C for 5 min
 19 followed by 95° C for 5 min. Then, the photoresist was exposed to UV light (J500IR/VISIBLE, MA6/BA6 Semi-automatic
 20 Mask Aligner, Suss Microtec, Germany) through the mask for 9 s. Next, the wafer was baked for post exposure bake at 65°
 21 C for 1 min followed by 95° C for 2 min. Further, to obtain the SU8 pattern on top of silicon master, UV-exposed wafer was
 22 developed for around 2.5 to 3 mins with SU8 developer. And finally the wafer was placed in oven at 100° C for 30 min to
 23 further improve adhesion between photoresist and wafer. Fig. S3 shows the microscopic image of the fabricated Si-master.
 24 After obtaining the silicon master, PDMS monomer and curing agent (sylgard- 184, Silicone Elastomer kit, Dow corning,
 25 USA) were mixed at mixing ratio 10:1 and it was poured onto the Si-master after degassing in the desiccator to remove air
 26 bubbles trapped during mixing. It was then cured inside a vacuum oven at 80° C for 45 mins. Once it is cured, the hardened
 27 PDMS layer which contains the channel structure was peeled off the silicon master and cut to size. Further, a 1.5 mm biopsy
 28 punch (shoney Scientific, Pondicherry, India) was used to punch fluidic access holes for the inlet and the outlet. To complete
 29 the channel of the device, PDMS layer containing channel was bonded to a glass slide using oxygen-plasma bonding (Harrick
 30 Plasma, Brindley St., USA). Finally, PTFE tubings (Instech Laboratories, PA, USA) were glued to the access holes to
 31 establish fluidic connection.



32
 33 **Fig. S3** Microscopic image of Si-master showing a single micro-constriction of cross-section $10.5 \times 10.5 \mu m$.

34

1 S.3 Cell preparation protocol

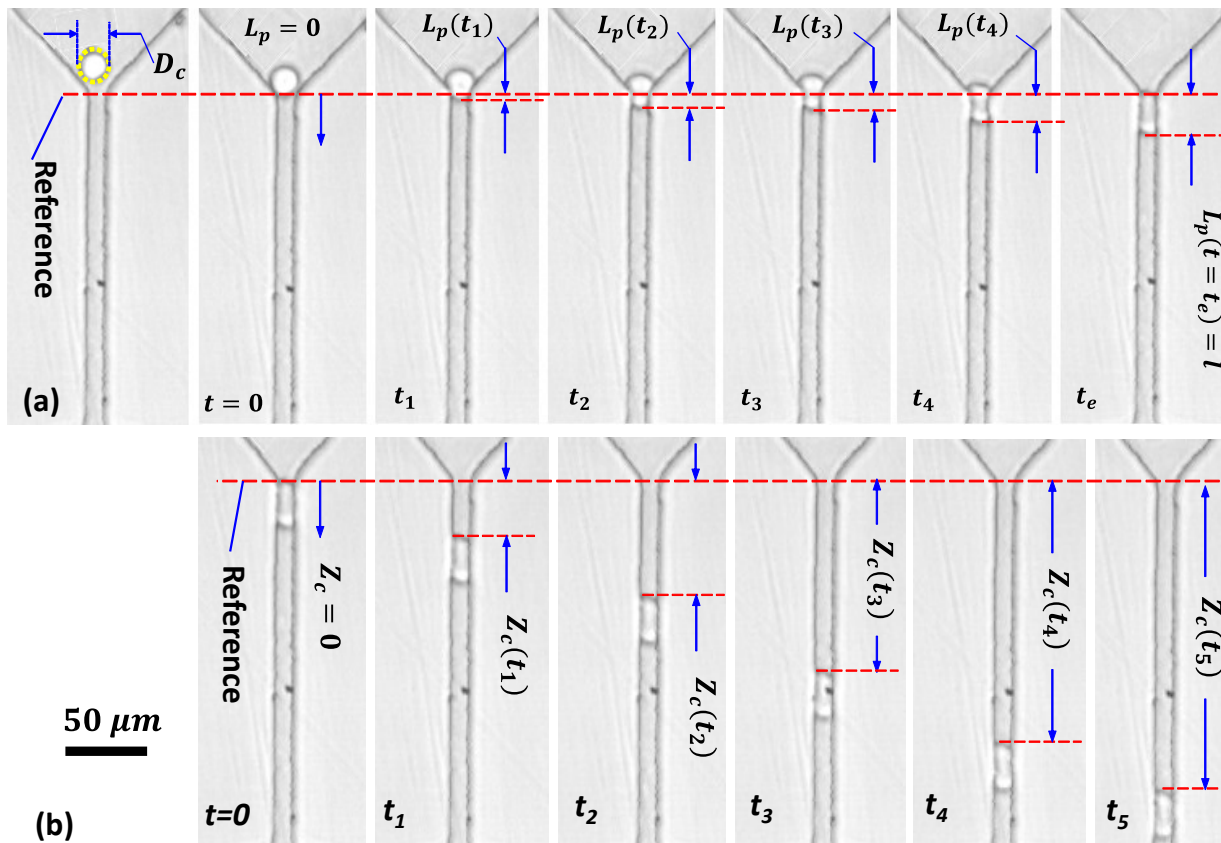
2 The cell lines (National Centre for Cell Sciences, Pune, India) kept at -80°C were revived, cultured into T-25 flask in
3 Dulbecco's Modified Eagle Medium (DMEM) (Himedia, India), which contained 20% fetal bovine serum and antibiotic mix
4 (50 mg gentamicin, 100 mg streptomycin, and 62.77 mg penicillin), and were incubated in CO_2 incubator. When the cells
5 were grown to confluence, the media was removed and the cells were washed thrice with Phosphate Buffered Saline. Then,
6 PBS was removed completely and trypsinized with 1X trypsin and incubated for 2-3 min in CO_2 incubator. The trypsinized
7 cells were added with 1.0 mL DMEM and then transferred into 15 mL Falcon tube and centrifuged for 5 min at 1800 rpm.
8 After centrifugation, the supernatant was removed and 1.0 mL of fresh media was added to the pellet. Then, the cells were
9 gently re-suspended. 1% Pluronic (BASF, Sigma –Aldrich, USA) was then added to the cell suspension before infusing into
10 the microfluidic device so as to reduce the adhesion between cell-cell and cell-wall. The average cell diameter of various
11 cells were ranging from 13 to 21 μm for all our experiments. The variation in the cell sizes were observed to be $\pm 0.6 \mu\text{m}$,
12 $\pm 1 \mu\text{m}$, $\pm 0.5 \mu\text{m}$ and $\pm 1.5 \mu\text{m}$ for 13 μm , 16 μm , 18 μm and 21 μm respectively.

13 For studies involving pharmacological treatments, 50 μM 4-Hydroxyacetophenone (4-HAP) (Spectrochem Pvt. Ltd, Mumbai,
14 India) solution with DMSO (Dimethyl sulphoxide, Himedia, India) was utilized. Cell samples were first treated with the 4-
15 HAP solution in DMSO for 30 min before infusing into the microfluidics device.

16 S.4 Experimental Procedure

17 As already explained in the section 3 and S.1.3, MFCS-EZ constant pressure based flow controller system along with s-type
18 flow unit sensor was utilized to infuse the cell sample into the microfluidic device. This system is capable of infusing the
19 sample with a pressure resolution of 1.0 mbar.

20 Before starting the experiments, the device microchannel was filled with a solution of 1% Pluronic (BASF, Sigma –Aldrich,
21 USA) with PBS (phosphate-buffered Saline, Germany, Sigma Aldrich) in order to coat the PDMS surface to avoid any
22 unspecific cell adhesion onto the channel walls. Then, the cell suspension (2×10^5 cells per mL of media with 1% Pluronic,
23 BASF) is infused into the device at a constant known pressure and the cell migration through the micro-constriction was
24 monitored and captured using Inverted microscope (Carl Zeiss Axiovert A1) coupled with a high-speed camera (FASTCAM
25 SA3 model, Photron USA, Inc.) interfaced with PC via Photron Fastcam Viewer 3 software (PFV3). We have used 20X
26 magnification objectives for our experiments. The cell migration videos were recorded at 3000 frames per second (fps) with
27 a resolution of 512×512 pixels. By using a 20X objective, the field of view was approximately 0.9 mm.



1
2 **Fig. S4** Schematic for image analysis of (a) entry process of a single cell (b) transit process of a single cell.

3 S.5 Image analysis & Data extraction

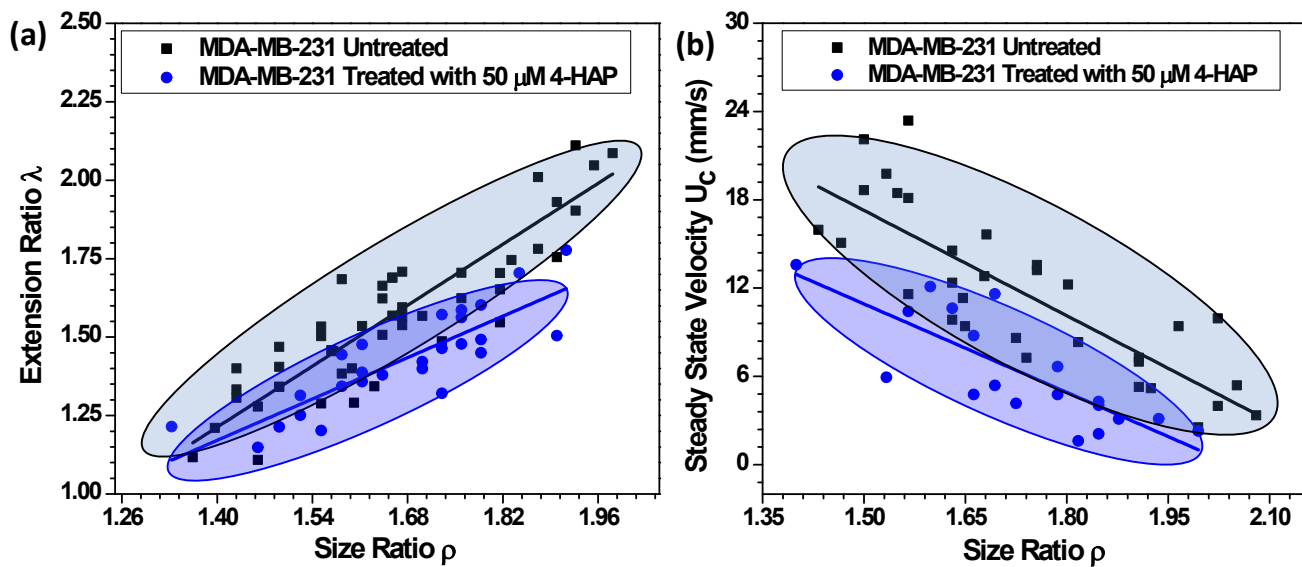
4 The videos taken for capturing the cell migration through micro-constrictions were analysed using Photon FASTCAM
 5 Analysis (PFA) software (Motion Analysis Software Version 1.3.2.0, Photron USA, Inc.), which tracks the movement of the
 6 cell surface (or any interface assigned) with time and finally plots the cell position along the length of the microchannel.
 7 Further, the same plot is utilized to obtain the migration velocity of the cell. The detailed procedure of the image analysis is
 8 explained as follows. As explained in the device description section of the manuscript, the entry time t_e is defined as the time
 9 duration in which cell completely squeezes inside the micro-constriction. Fig.S4 (a) shows the step by step analysis of images
 10 to deduce the entry time. The images from left to right shows the successive protrusion $L_p(t)$ of a single cell with time. The
 11 leftmost image shows the cell before entering into the micro-constriction. We measure the diameter of the cell by fitting the
 12 visible cell surface with a circle. We have taken 3 to 5 reading for each given single cell in order to get more reliable data and
 13 used the average value for the analysis. The starting edge of the micro-constriction was taken as reference for further
 14 measurements (shown by a red dashed line). At time $t=0$, cell protrusion into the micro-constriction starts and hence
 15 $L_p=0$. The leading edge of the cell was tracked with time and protrusion length L_p was measured with time. Finally when
 16 cell completely squeezes inside, $L_p=l$, time duration $t=t_e$ is noted down as entry time. Thus, cell protrusion $L_p(t)$ gets
 17 monitored with time and entry t_e is obtained.

18 Further, for the analysis of the transit behaviour of cells, a fixed reference position and time was used. The point of time,
 19 when a cell has completely squeezed inside the micro-constriction is represented as $t=0$ (Leftmost image of Fig. S4(b)).
 20 Images from left to right show the positions of the cell $Z_c(t)$ along the micro-constriction at different time instants
 21 t_1, t_2, t_3 and so on. Since, there is no significant change in the cell deformation further, the rear edge of the cell was monitored
 22 with time. Once, $Z_c(t)$ is measured at different time instants, we obtain the plot $Z_c(t)$ vs. time, which is further used to obtain

1 the cell velocity variation along the channel. *PFA* software is capable of monitoring an assigned cell surface (leading edge in
2 the case of entry time analysis and rear edge in the case of transit behaviour analysis) and plot the graphs automatically.

3 S.6 Pharmacological treatment of cell and results

4 As explained in the section 4.6, in order to characterize our device (along with model) for pharmacological treatments, we
5 have treated MDA-MB-231 cells with $50 \mu\text{M}$ 4-Hydroxyacetophenone (4-HAP) solution for 30 mins before infusing the cells
6 into the channel. Fig. S5 (a) and (b) respectively shows the comparison of the extension ratio and the steady state velocity of
7 the treated cells with the untreated one. Fig. S5 (a) shows a decrement in the extension ratio of the cell because of the
8 treatment, thus confirming a stiffening of the cell. Similarly, the steady state velocity U_c also decreases with the treatment
9 (fig. S5 (b)).



10
11 Fig. S5 (a) Comparison of extension ratio of MDA-MB-231 cells before and after the treatment (b) Comparison of steady
12 state velocity of MDA-MB-231 cells before and after the treatment, applied pressure across the micro-constriction is 100
13 mbar.

14

15 References

- 16
17 1 M. A. Tsai, R. S. Frank and R. E. Waugh, *Biophys. J.*, 1993, **65**, 2078–2088.
18 2 H. Lamb, 1945, *Dover Publ. New York*.
19 3 S. Byun, S. Son, D. Amodei, N. Cermak, J. Shaw, J. H. Kang, V. C. Hecht, M. M. Winslow, T. Jacks, P. Mallick
20 and S. R. Manalis, *Proc. Natl. Acad. Sci. U. S. A.*, 2013, **110**, 7580–5.
21 4 L. M. Lee and A. P. Liu, *Lab Chip*, 2015, **15**, 264–273.
22 5 J. R. Lange, J. Steinwachs, T. Kolb, L. A. Lautscham, I. Harder, G. Whyte and B. Fabry, *Biophys. J.*, 2015, **109**,
23 26–34.
24